Determination of HISCALE MFSA Background Rates Using IMP-8 Monitored Omnidirectional Galactic Cosmic Rays

20th February 2001

J. D. Patterson and T. P. Armstrong
Fundamental Technologies, LLC, Lawrence, KS

Abstract

In this short work, we provide clear evidence that the background rates for the EPAM and HISCALE MFSA data are in large part caused by galactic cosmic rays. We also present a method by which the background rates as a function of time may be determined for the EPAM and HISCALE instruments using the integral high-energy charged particle flux ($E > 60\ MeV$) as measured by the IMP-8 CPME instrument. Finally, we also present a means of determining the contributions made by the RTG gamma rays to the overall HISCALE background rates. These data and analyses are preliminary. More work on this issue is underway and the final results will be made available as soon as possible.

INTRODUCTION

The Ulysses Heliospheric Ion Spectra and Composition Analysis at Low Energies (HISCALE) and Advanced Composition Explorer (ACE) Electron Proton Alpha Monitor (EPAM) detector assemblies rely upon singles rates in simple detector assemblies in order to observe the energy spectra of $E > 30$ keV electrons and ions. At higher energies, above 400 keV, multiple detector coincidences are used to define more selective passbands for ions. Nevertheless, the singles channels are much more sensitive, having larger geometrical factors and lower energy thresholds. Accurate determination of the "out of nominal passband" response, aka "background," is critical to extracting the maximum information from both HISCALE and EPAM. The EPAM and HISCALE instruments utilize five telescopes to collect the data mentioned above, the composition aperture (CA), two low-energy magnetically shielded (LEMS) telescopes, and two low-energy foil shielded (LEFS) telescopes. A schematic of the detector assemblies for EPAM and HISCALE is shown below in Figure 1.

Figure 1: LEMS, LEFS and CA telescope assemblies for EPAM and HISCALE.

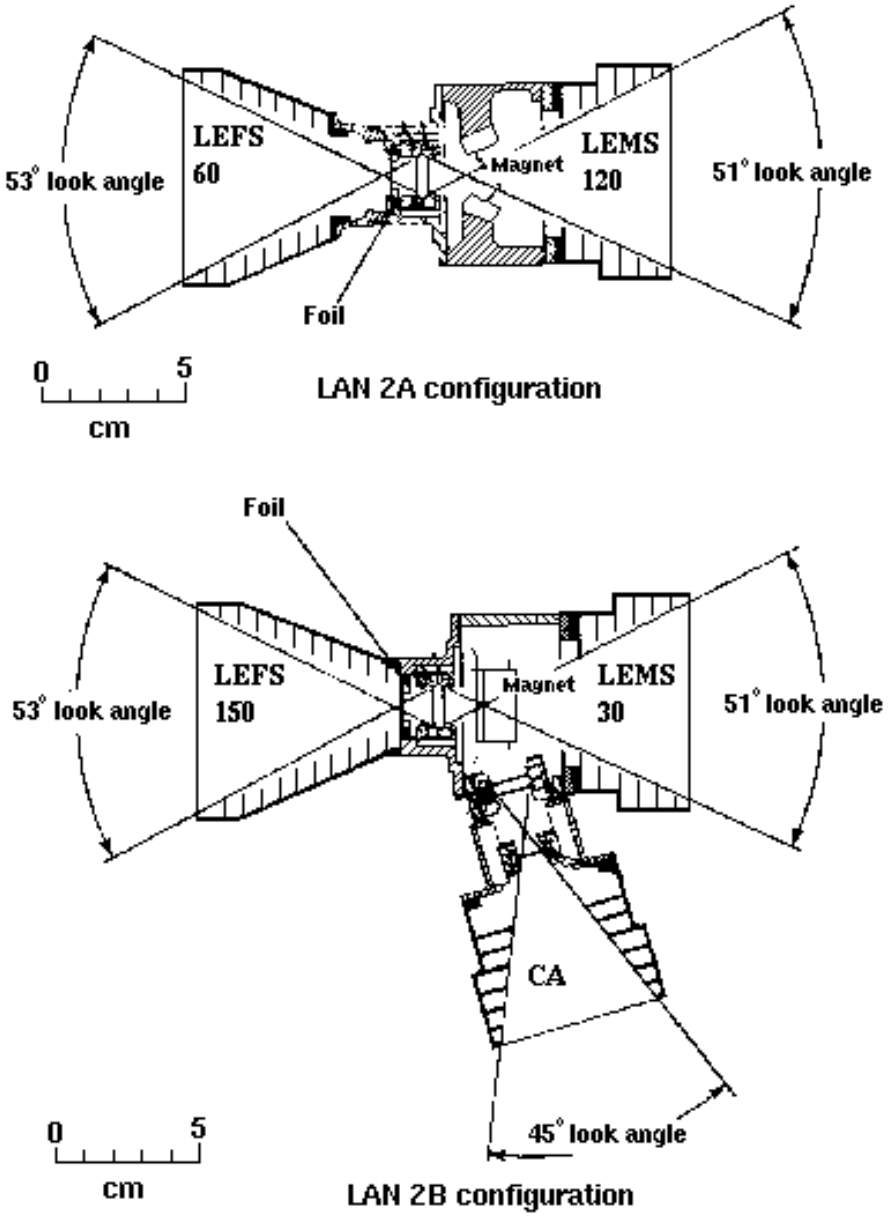

Figure 2: Time series of IMP-8 $E>60$ $MeVs$

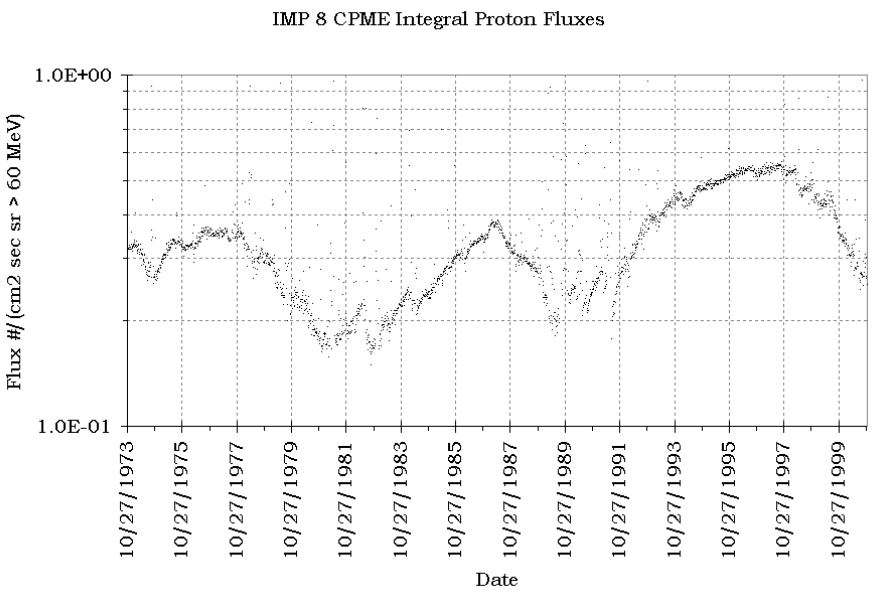

The problem of finding the correct background values for the MFSA data from HISCALE and EPAM has been studied for some time. Some early work on the issue was done by *Simnett* [1994] and *Tappin* [1994]. One of the simplifications in previous attempts to determine the background rates has been the assumption that these rates are constant. They are not. The major contributors to the background rates in the HISCALE and EPAM MFSA data are galactic cosmic rays (GCR). The GCRs are, of course, modulated by the 11-year solar cycle. Figure 2 shows the effect of this modulation very well. The clustering of low fluxes, daily averaged, shows the background. Note that these rates are largest in 1976, 1986, and 1996 (sunspot minima), and lowest in 1980, 1988, and 2000 (sunspot maxima). The result of this modulation, as it affects EPAM and HISCALE, is to alter the level of the background levels of the MFSA data. The background rates seen in EPAM and HISCALE should be greater during quiescent periods than during periods of high activity.

The most common method used to determine the background rate is to examine the raw data and search for low, slowly varying or nearly constant rates. This method greatly restricts the range of times for which the background rates can be known. The method that we have employed and that we describe here is a method by which the foreground rates are determined through independent means and subtracted from the MFSA data. This results in a first approximation of the background counts. The major benefit to this method is that it can be employed at all times. This results in a much more complete time series of background corrected rates.

COMPUTATIONAL METHODS

This method is based on the process of calculating the known contributions to the MFSA rates. The MFSA rates are singles with anticoincidence conditions to establish that the energies measured are the total energies of stopped particles [M' ~F', M ~F, F ~M, F' ~M']; see Figure 1. The first step is to use the composition aperture (CA) channels W1 and W2 to determine the number of counts that occur in the LEMS MFSA channels that correspond to the total energies of the protons that W1 and W2 measure. Figure 3 shows the MFSA energy calibration compared to the W1 and W2 passbands. Note that the W1 passband, 0.480 to 0.966 MeVs, corresponds to MFSA channels 19.5 to 23.42, and the W2 passband, 0.966 to 1.40 MeVs, corresponds to MFSA channels 23.2 to 24.3. Table 1 contains the energy thresholds and geometric factors for these channels. The same passbands are valid for both the EPAM and the HISCALE instrument. We call these numbers interpolated from the observed MFSA counts *LW1* and *LW2*, respectively. The WART data are known to be solely protons, and, as a result of the detector's coincidence logic, virtually free of background. This enables the independent determination of the number of protons present at a given time. The W1 and W2 data are compared to the integral rates in the corresponding MFSA energy channels, adjusted for the different passbands and geometric factors of the detectors, of course. Let us call this rate *LW1* and *LW2*, for the "*L*EMS predicted *W1* and *W2* counts." *LW1* and *LW2* are calculated in the following manner:

$$\begin{aligned} LW1 \;=\; & \left[\left(\frac{E_{19,high}-E_{W1,low}}{E_{19,high}-E_{19,low}}\right)\cdot MFSA_{19}+MFSA_{20}+MFSA_{21}\right. \\ & \left.+MFSA_{22}+\left(\frac{E_{W1,high}-E_{23,low}}{E_{23,high}-E_{23,low}}\right)\cdot MFSA_{23}\right]\cdot\left(\frac{g_{W1}}{g_{LEMS}}\right), \end{aligned} \tag{1}$$

$$\begin{aligned} LW2 \;=\; & \left[\left(\frac{E_{23,high}-E_{W2,low}}{E_{23,high}-E_{23,low}}\right)\cdot MFSA_{23}\right. \\ & \left.+\left(\frac{E_{W2,high}-E_{24,low}}{E_{24,high}-E_{24,low}}\right)\cdot MFSA_{24}\right]\cdot\left(\frac{g_{W1}}{g_{LEMS}}\right), \end{aligned} \tag{2}$$

where the subscripts refer to the MFSA channel number. There are several contributions to the MFSA rates within this range of energies: protons, foreground $Z>1$ particles, and GCR-induced background. These contributions are summarized in the following two equations:

$$LW1 = W1_{Z=1} + LW1Z2_{Z>1} + LW1b_{GCR} \tag{3}$$

$$LW2 = W2_{Z=1} + LW2Z2_{Z>1} + LW2b_{GCR} \tag{4}$$

Table 1: Energy passbands and geometric factors for the HISCALE channels used by this study [*Armstrong*, 1999].

Channel	$E_{low}(keV)$	$E_{mid}(keV)$	$E_{high}(keV)$	$g(cm^2sr^1)$
W1	480.0	680.9	966.0	0.103
W2	968.0	1079.6	1204.0	0.103
Z2	668.0	1875.2	5264.0	0.279
$MFSA_{19}$	431.224	474.842	522.872	0.428
$MFSA_{20}$	522.872	575.798	634.081	0.428
$MFSA_{21}$	634.081	698.311	769.048	0.428
$MFSA_{22}$	769.048	847.013	932.881	0.428
$MFSA_{23}$	932.881	1027.53	1131.79	0.428
$MFSA_{24}$	1131.79	1246.73	1373.35	0.428

The result is that the equivalent MFSA rates, *LW1* and *LW2*, exceed the measured *W1* and *W2* rates because *LW1* and *LW2* have both $Z>1$ and background contributions. Subtracting *W1* and *W2* from *LW1* and *LW2* yields the counts in *LW1* and *LW2* that are not resulting from protons within the 0.5 to 1.2-MeV range.

Although after subtraction the counts in the MFSA data that are not the result of protons is known, these counts are still not all resulting from the background GCRs. The LEMS detectors are also sensitive to alpha and $Z>2$ particles. The Z2 channel records counts from $Z>1$ particles. However, the Z2 passband is very broad, having a lower energy threshold of 668 keV and an upper energy threshold of 5264 keV, and is not conveniently segmented into energy ranges as the WART data are. The solution to this is to make the assumption that the spectral exponent for the $Z>1$ particles is the same as for protons. From this, a power-law function can be determined for $Z>1$ particles using the Z2 rate data.

$$Flux_{Z>1} = A_{Z2}E^{\gamma} \tag{5}$$

$$Z2 = \frac{A_{Z2}}{\gamma+1}\left(E_{Z2,high}^{(\gamma+1)} - E_{Z2,low}^{(\gamma+1)}\right) \tag{6}$$

$$\Longrightarrow A_{Z2} = \frac{Z2\cdot(\gamma+1)}{\left(E_{Z2,high}^{(\gamma+1)} - E_{Z2,low}^{(\gamma+1)}\right)} \tag{7}$$

where γ is found using *LW1* and *LW2* in the following manner:

$$\gamma = \frac{log\left(\frac{LW1}{LW2}\right)}{log\left(\frac{E_{W1,mid}}{E_{W2,mid}}\right)} \tag{8}$$

The above equation for *Z2* can now be solved to find the flux constant, A_{Z2}. With A_{Z2} and γ known, the $Z>1$ rates in *LW1* and *LW2*, *LW1Z2* and *LW2Z2* respectively, can be calculated as follows:

Figure 3: MFSA energy passbands and the correspondence to the W1, W2, and Z2 energy passbands.

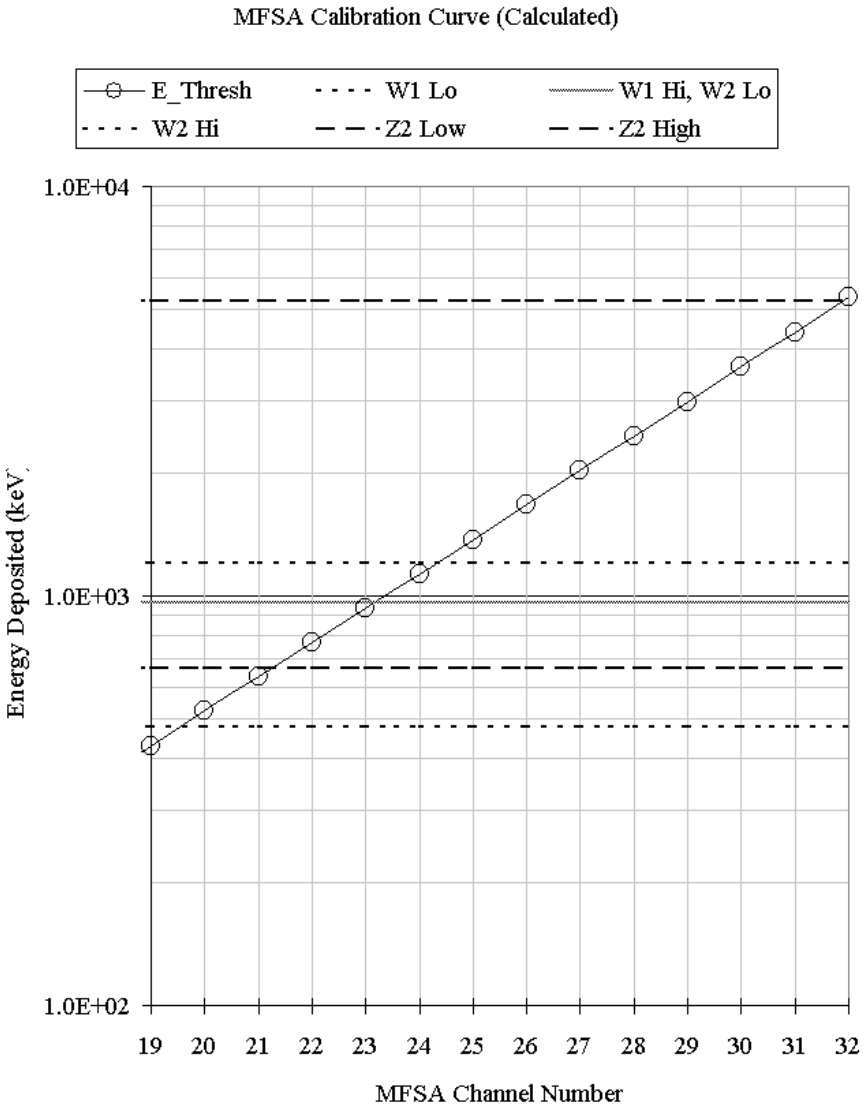

$$LW1Z2 = \frac{A_{Z2}}{\gamma+1}\left(E_{W1,high}^{(\gamma+1)} - E_{W1,low}^{(\gamma+1)}\right) \cdot \left(\frac{g_{W1}}{g_{Z2}}\right) \tag{9}$$

$$LW2Z2 = \frac{A_{Z2}}{\gamma+1}\left(E_{W2,high}^{(\gamma+1)} - E_{W2,low}^{(\gamma+1)}\right) \cdot \left(\frac{g_{W1}}{g_{Z2}}\right) \tag{10}$$

Subtracting the $Z>1$ counts from *LW1* and *LW2* finally results in the true background rates, at least within the range of energies represented by MFSA channels 19 through 24, *LW1b* and *LW2b*.

$$LW1b = LW1 - W1 - LW1Z2 \tag{11}$$

$$LW2b = LW2 - W2 - LW2Z2 \tag{12}$$

The resulting values for *LW1b* and *LW2b* stand on their own logically, but separate verification of these results is certainly preferable. Such verification is obtainable through the Charged Particle Measurement Experiment (CPME) instrument on-board the Interplanetary Monitor Platform (IMP-8). IMP-8 is in Earth orbit at an average distance of $\sim 30R_E$ [*Armstrong*, 1976]. Although Ulysses and IMP-8 are not flown in the same region of the heliosphere, the GCR flux measured by IMP-8 does an excellent job of predicting the magnitude of the *LW1b* and *LW2b* values calculated above. Figure 4 compares the raw time-series of IMP-8's P11 (145 MeVs$<E_p<$440 MeVs) and the *LW1* and *LW2* data. The only difference between the three time series is a constant multiplicative factor. At the energies for which the above analysis is done, the only contributor to the background is assumed to be GCRs, since the modeled RTG induced rates fall off rapidly past MFSA channel 18 [*Gomez*, 1996]. Therefore, the IMP-8 data serve as great indicators of the high-energy MFSA background as seen in Figure 4. One very critical assumption that must be made in comparing the two data sets is that the forground flux of particles for the MFSA and CA data are isotropic. This analysis hinges upon the flux of particles seen by LEMS30, LEMS120, and the CA being identical. The spikes in the *LW1b* and *LW2b* values seen in Figure 4 are the result of anisotropic events. For the determination of background rates, these spikes can be safely ignored since they are obviously the result of foreground activity.

It was determined that the *LW1b* values were 50% of the IMP-8 P11 flux. Although a similar multiplicative factor could also be used to model the *LW2b* value, we instead chose to use a standard spectrum for the background rates, and use the *LW1b* value to determine the *LW2b*. The premise was that if the modeling of *LW2b* was successful in its agreement with the observed data, the assumption of the type of energy spectrum for the background rates is valid.

The model for the GCR component to the overall MFSA background spectrum was obtained from quiescent EPAM data. The assumption that was made at this point was that the shape of the background spectrum would remain unchanged as the overall flux of GCRs increases or decreases, so that the time variance of the background rates is unimportant at this step. The shape of

Figure 4: Time series of IMP-8 E>60 $MeVs$, W1, and W2

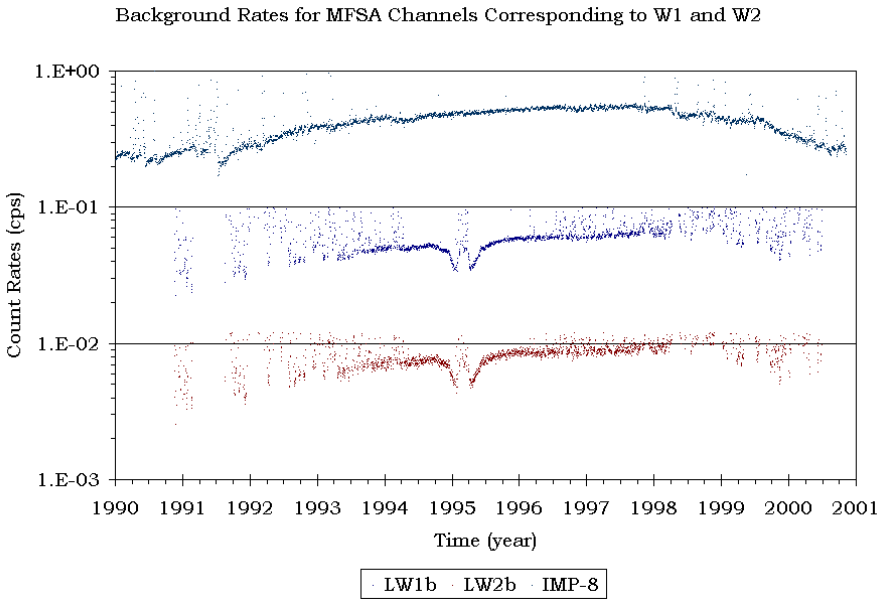

Table 2: Fit parameters for the modeling of EPAM background rates.

Parameter	Value
a	5000
b	-23.5
c	1.69
d	23.9
e	-0.897
f	-0.00174

the EPAM background spectrum during days 359 to 362 of 1997 was found to resemble the following curve:

$$R_{EPAM-background}(E,t) = A(t) \cdot \left[\frac{a}{(E-b)^c \cdot exp\left(\frac{d}{E-b}\right) - e} - f \right], \qquad (13)$$

where A is a normalization factor to be determined later. For the range of dates given above, and A=1, the values for the parameters, a through f, are presented in Table 2. The resulting model spectrum and the data upon which it is based are shown in Figure 5.

This mathematical description was used as a basis to determine the background spectra for times throughout the Ulysses mission. To do this, the model

Figure 5: EPAM Background Rates for Days 359 to 362 of 1997 and the modeled GCR contribution to the MFSA background spectrum.

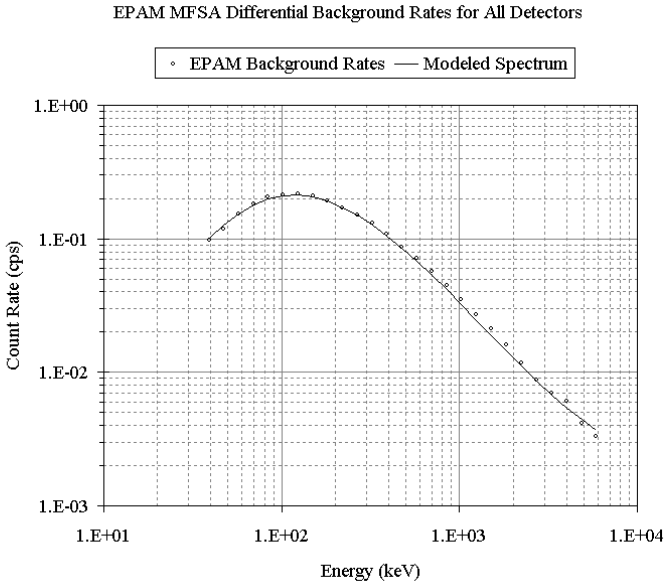

spectrum was integrated over the W1 passband, and was compared to 50% of the IMP-8 rates. The ratio of the integrated spectrum and 50% of the IMP-8 rates, therefore, serves as the normalization, A, for the time-varying GCR-contributed background spectra. The test of this method is to check that it predicts the correct value of *LW2b*. Figure 6 shows the result of these calculations and comparisons. It is evident from the graph that the predicted values of LW2b are in excellent agreement with the measured values. The sole place in which there is significant discrepancy is during the time of Ulysses' passage through the streamer belts during the fast latitude scan in the early part of 1995. During this time, the GCRs at the location of Ulysses were heavily modulated, whereas the GCRs at the location of IMP-8, $\sim$1 AU in the ecliptic, do not show this fluctuation. Notice also from the graph that when Ulysses does pass through the ecliptic at $\sim$1 AU, the measured value of *LW1b* and *LW2b* agree very well with the IMP-8 data. We focus on this feature in a paper to be presented in the near future.

For the HISCALE instrument, as opposed to EPAM, the GCRs are not the only major contributor to the background rates. The gamma ray spectrum from the radiothermal generators (RTGs) also add to the background noise. To determine the RTG contribution to the in-flight background rates, the modeled GCR contribution to the background rates was subtracted from the rates obtained during periods of low activity. A few quiet periods were selected from 1993, 1996 and 1997 for this: days 115 to 120 of 1993, days 257 to 273 and

Figure 6: Modeled *LW1b* and *LW2b* based upon the IMP-8 P11 rates for 145 MeVs$<E<$440 MeVs protons and the modeled EPAM background spectrum.

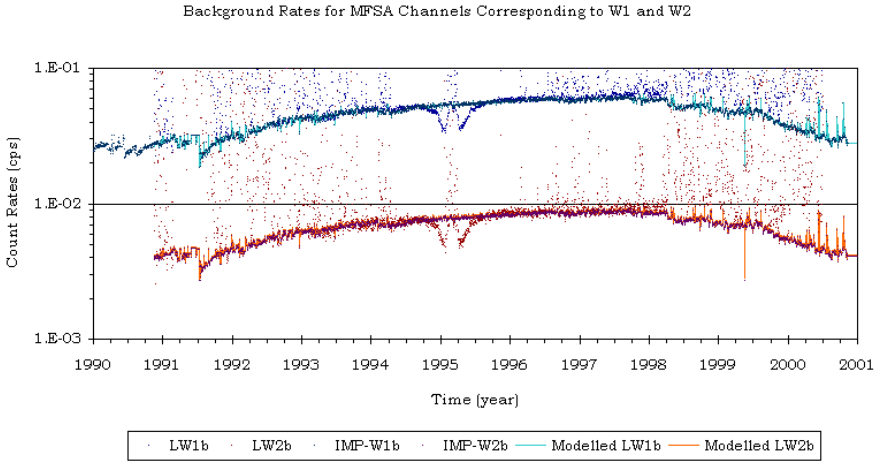

303 to 323 of 1996, and days 161 to 167 of 1997. Since the time rate of change in the RTG gamma ray spectrum is slow, and the orientation of the RTGs to the HISCALE instrument is always the same, there should be no observable time variance in the RTG contribution to the MFSA data. Figure 7 depicts the resulting average RTG contribution to the MFSA background rates.

RESULTS

There have been a number of attempts to model the HISCALE response to the RTG gamma rays, most notably a study by *Gomez* [1996]. In this study, the RTG gamma ray spectrum was assumed to be the same as it was when the RTGs were analyzed in the lab prior to launch. To be sure, the gamma ray spectrum of the radioisotopes used in the RTG does change over time, but not at a significant enough rate to be a problem. Gomez applied a Monte Carlo method of tracking the gamma rays through the silicon wafer used by the HISCALE detectors. The result of his work was a normalized modeled contribution by the RTG gamma rays to the overall background rates in the MFSA data. These results are summarized in Figure 8 below.

This modeled RTG contribution assumes a bare detector with direct exposure to the RTG gamma rays. This is not the case. Various hardware exists between the RTGs and the HISCALE detectors on the actual spacecraft, and this has the effect of subtly altering the incident gamma ray spectrum. A preflight study was done to gain an experimental estimate of the RTG contribution to the MFSA counts. The flight certified RTG assembly was placed with the complete HISCALE assembly in a vacuum chamber in the same relative posi-

Figure 7: RTG contribution to the HISCALE MFSA data based upon the subtraction of the modeled GCR contribution from the total count rates during selected quiescent times.

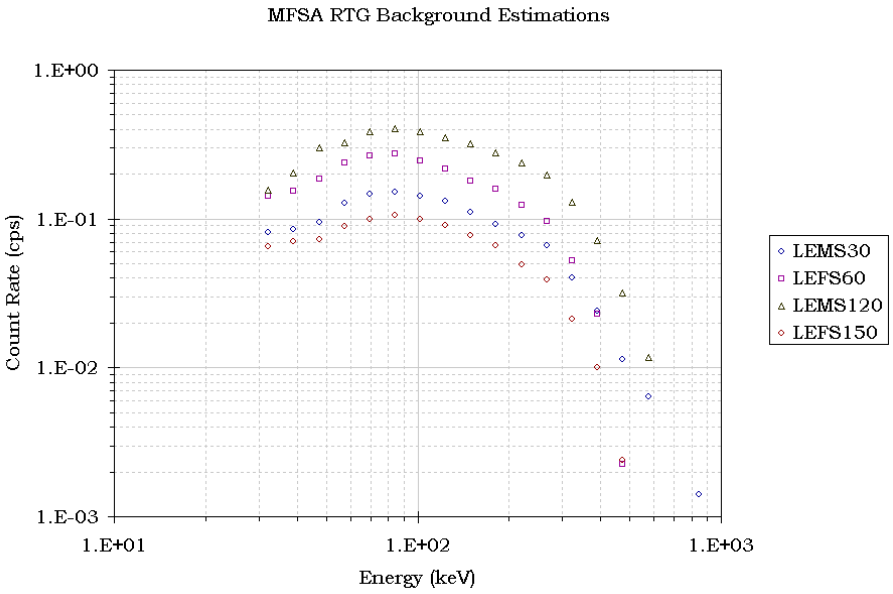

Figure 8: Normalized MFSA rates for both a vertically incident and an obliquely incident RTG gamma ray spectrum. [*Gomez*, 1996]

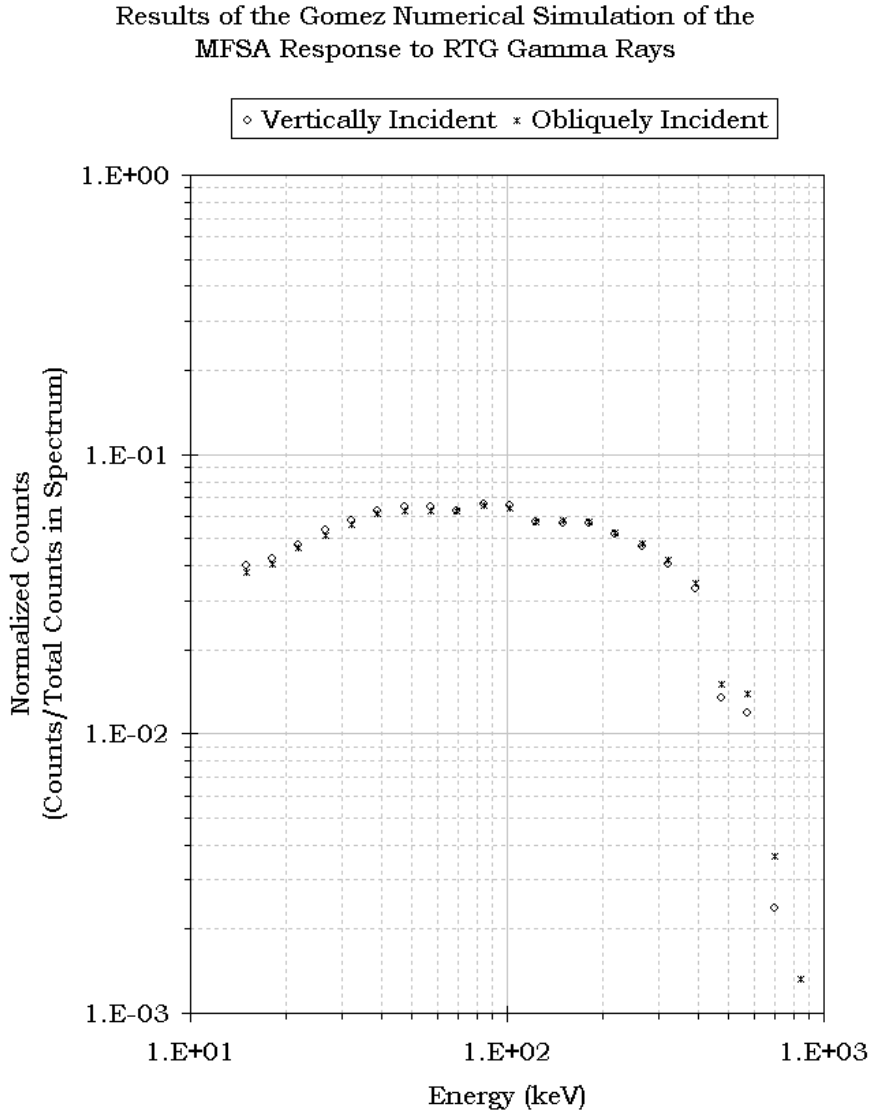

tions as they would later occupy when attached to the Ulysses spacecraft. Two accumulations were taken, one with the two instruments in air and the other with the two instruments within a vacuum [*Gold*, 1984]. The results of these 128-second, sector-averaged, measurements are shown in Figure 9.

These results compare favorably, when normalized, to the rates predicted by *Gomez* [1996] and the preflight laboratory measurements. The comparison between the RTG-induced rates, shown in Figure 7, the rates predicted by *Gomez* [1996], shown in Figure 8, and the preflight laboratory measurement [*Gold*, 1984], shown in Figure 9, is given in Figure 10.

The very close agreement between the preflight measurement of the RTG contribution to the total MFSA background rates and the contribution as determined by this present study confirms the validity of the method of computing the MFSA background rates over all energies outlined by this present study.

CONCLUSIONS

From the results presented in the above section, we draw the following conclusions:

1. The main contributors to the HISCALE background rates in all energy channels are GCRs of energy 145 to 440 MeVs and perhaps greater.

2. Secondary contributors to the HISCALE background rates in energy channels below about 500 keVs are gamma rays from the RTG.

3. The RTG contribution to the background rates is time-independent.

4. The GCR contribution to the background rate is time-varying in a manner predictable by measuring the GCR rates using the channel P11 of the CPME instrument on-board IMP-8.

5. The spatial variations in the GCR contributions are significant only during the fast latitude scan portion of the Ulysses orbit.

The very close agreement between the IMP-8 measured GCRs and the estimated high-energy MFSA background rates, *LW1b* and *LW2b*, provides excellent evidence that the background rates seen in the MFSA data are induced by penetrating GCRs. This evidence is strengthened by the fact that the IMP-8 GCR data follows the time-variance of the *LW1b* and *LW2b* values so well. The only time during the entire Ulysses mission at which the IMP-8 data and the MFSA data do not follow the same time variance is during the fast latitude scan. This portion of the Ulysses orbit passes through streamer belts just above and below the solar equatorial plane. It is known that the GCRs are heavily modulated in this region and, therefore, the background rates can be expected to drop as the GCR flux drops. The modeling of this variation of the background rates can not be performed by the process presented in this paper, but an analysis of this phenomenon will be presented at a later date.

Figure 9: RTG contribution to the HISCALE MFSA data as measured by a preflight laboratory measurement [*Gold*, 1984].

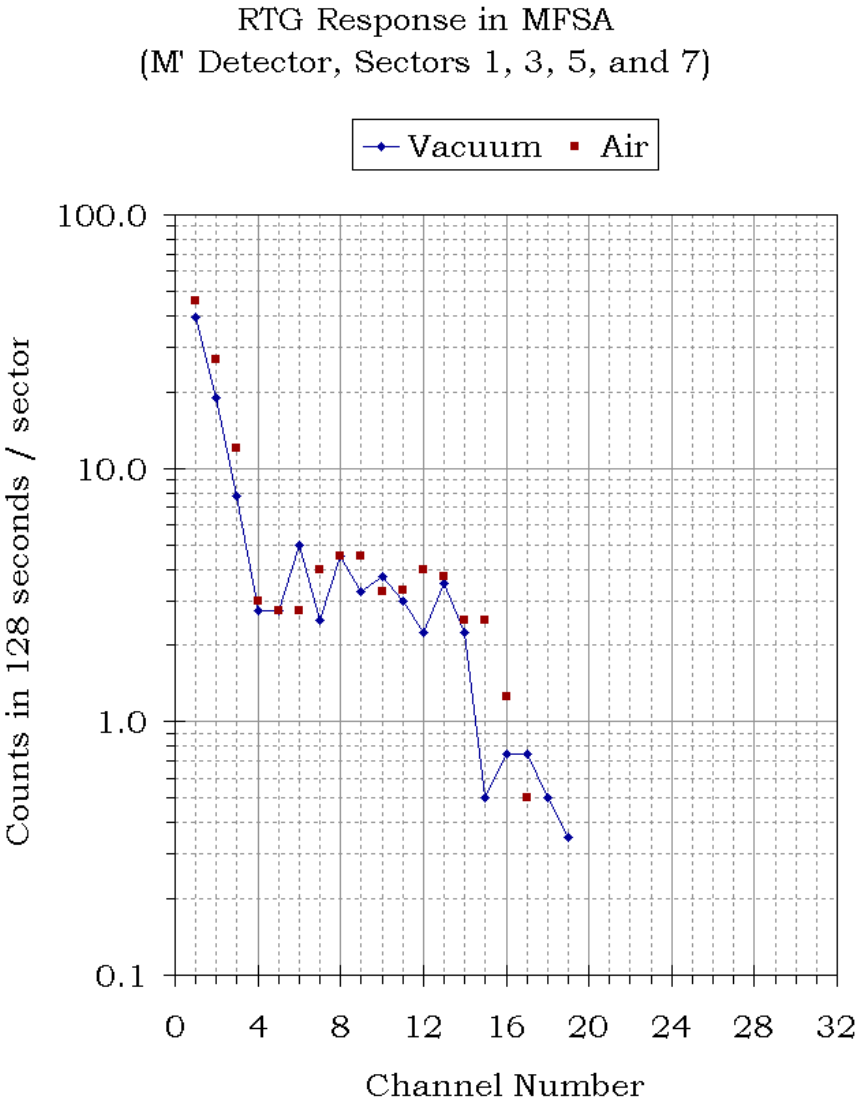

Figure 10: Comparison between the predicted RTG induced rates by *Gomez* [1996], the preflight laboratory measurement [*Gold*, 1984], and the RTG induced rates as determined by this present study.

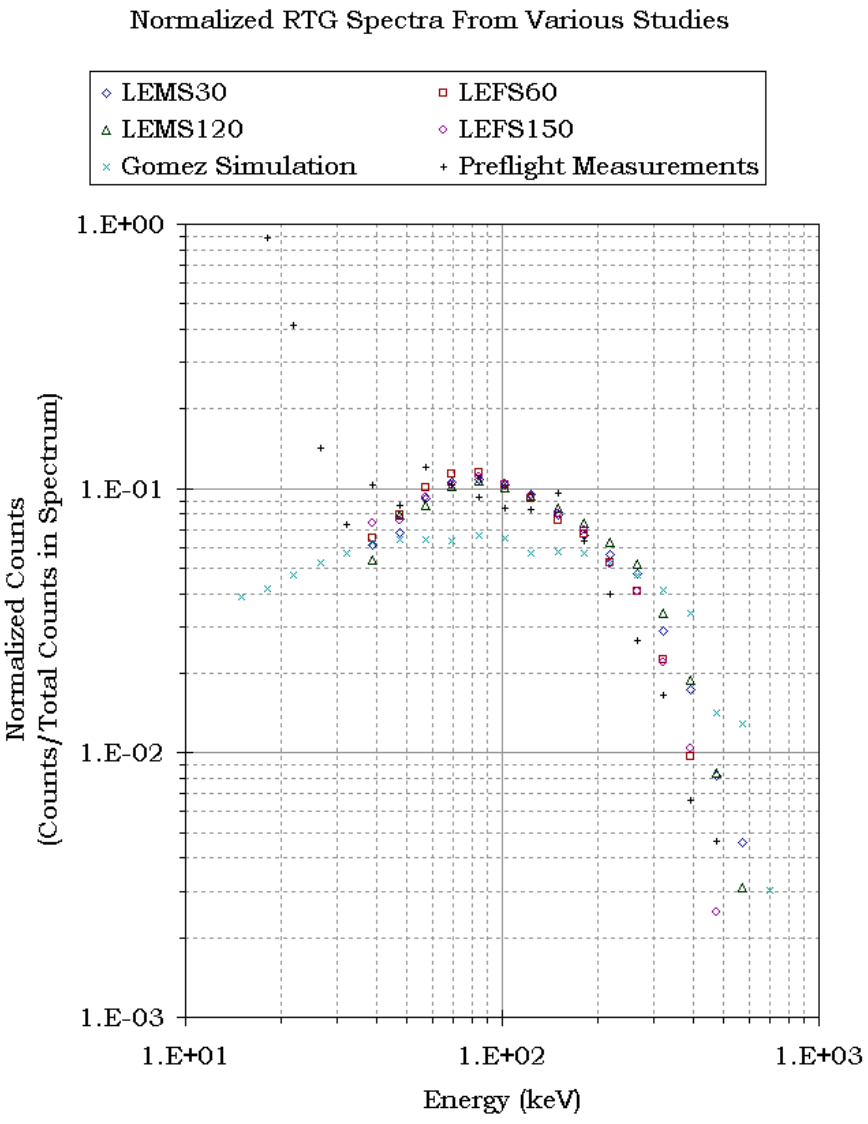

At energies less than ~500 *keVs*, below MFSA channel 20, the RTG gamma rays also contribute strongly to the background rates in the MFSA data. At higher energies, the RTG contribution diminishes rapidly. This concurs with the measured results from the preflight laboratory test and with the numerical simulation made by *Gomez* [1996]. These RTG-induced rates are essentially time-independent. Although the emitted gamma ray spectrum of the RTG changes over time as the plutonium fuel decays, the overall energy flux, and therefore the total energy striking the detector, changes minimally if at all. No trend over time was noticed in this study and we conclude that the assumption of a time-independent RTG contribution to the total background counts is a safe one.

ACKNOWLEDGMENTS

The authors would like to express their thanks to the work and labor of the HISCALE team on previous efforts to address the problem of determining background rates for the HISCALE detector. Much of this present study was made possible only by their efforts. This work was made possible by funding from NASA Grants #NAS5-97271 and #NAG5-6113.

References

[1] Armstrong, T. P., Handbook and reference manual for charged particle measurement experiment data from Explorer 47 and 50, John Hopkins University Applied Physics Laboratory, 1976.

[2] Armstrong, T. P., Hunt-Ward, T. ed., Ulysses HISCALE data analyses handbook, internal document, Fundamental Technologies, 1999.

[3] Gold, R. E., RTG radiation background tests, memo to the HISCALE Instrument Team, 1984.

[4] Gomez, J., Monte Carlo simulation of MFSA response to RTG gamma rays, internal document, Fundamental Technologies, 1996.

[5] Simnett, G. M., Background analysis for the high latitude cosmic ray study, University of Birmingham, 1994.

[6] Tappin, S. J., HISCALE backgrounds, a new look, HISCALE internal document, 1994.